Prediction of Cerebral Hyperperfusion Syndrome After Combined Bypass Surgery in Moyamoya Disease Using Hemodynamic and Clinical Data

Min-Kyung Jung, MS, Eun Jin Ha, MD,*† Jin Hyung Kim, MS,* Young Sill Kang, MD, PhD,† Yuwhan Chung, MD,† Jeong Eun Kim, PhD,† Hakseung Kim, PhD,* Dong-Joo Kim, PhD,*‡ and Won-Sang Cho, MD, PhD†*

Purpose: Cerebral hyperperfusion syndrome (CHS) is a postoperative complication in moyamoya disease (MMD). However, limited studies have investigated the association between preoperative hemodynamic features and postoperative CHS. In this study, we aimed to identify the predictors of postoperative CHS in MMD using preoperative hemodynamic and clinical data.

Patients and Methods: In this retrospective study, we analyzed data from 72 hemispheres of 56 adult patients with MMD who underwent combined bypass surgery. Hemodynamic features were extracted from the region of interest on preoperative arterial spin-labeling magnetic resonance imaging and basal and acetazolamide-challenged single-photon emission computed tomography (SPECT). The predictive capacity of the hemodynamic features for postoperative CHS was analyzed using a generalized estimating equation. Multivariable analysis was performed using hemodynamic and clinical data.

Results: Postoperative CHS occurred in 35 operated hemispheres (48.61%). Univariable analysis revealed that the cerebrovascular reservoir capacity (CVR) in the temporal and frontal cortices on SPECT significantly predicted CHS, with a lower CVR observed in the CHS group ($P < 0.050$). In multivariable analysis, a lower CVR in the temporal cortex [odds ratio (95% CI), 0.99 [0.98–0.99]; $P = 0.034$], higher preoperative modified Rankin scale score [1.18 (1.05–1.33); $P = 0.008$], and anastomosis at the left hemisphere [1.25 (1.05–1.47); $P = 0.010$] were associated with an increased CHS risk.

Conclusions: Low preoperative CVR in the temporal cortex, poor preoperative neurological status, and surgery at dominant hemisphere are potential risk factors for postoperative CHS in MMD.

Key Words: moyamoya disease, cerebral hyperperfusion syndrome, bypass surgery, prediction, hemodynamic

(*Clin Nucl Med* 2025;00:000–000)

Moyamoya disease (MMD), an idiopathic cerebrovascular disease, is characterized by progressive steno-occlusion of the distal internal carotid arteries and compensatory development of fine abnormal vascular networks.[1] The underlying causes of MMD remain unclear; however, direct bypass surgery is considered effective in preventing the recurrence of ischemic and hemorrhagic events in adult MMD.[2–5] Nevertheless, complications such as cerebral hyperperfusion syndrome (CHS) after direct bypass surgery remain concerning because postoperative CHS can lead to severe sequelae unless properly managed.[6–9]

The mechanism underlying postoperative CHS remains controversial despite the recently reported potential candidates, including the occurrence of preoperative hypertension, high hematocrit levels, disruption of the blood-brain barrier and impaired cerebral autoregulation, low cerebrovascular reservoir capacity (CVR), free radicals, and metalloproteinase-9.[10–21] Clinicians have attempted to find significant hemodynamic features on radiologic images related to CHS, because such radiologic data are very effective to apply in clinical settings. However, only 1 study by Sato et al[17] indirectly demonstrated a significant hemodynamic effect of low preoperative CVR on postoperative CHS. This study aimed to predict postoperative CHS in adult patients with MMD undergoing combined bypass surgery by analyzing preoperative hemodynamic and clinical data.

PATIENTS AND METHODS

Study Population

Among adult patients who underwent extracranial-intracranial bypass surgery between November 2019 and June 2023, data collected from 72 hemispheres of 56 patients with adult ischemic MMD were included in this retrospective study (Fig. 1). The inclusion criteria were as follows: patients (1) diagnosed with MMD according to the Japanese guideline[10]; (2) aged ≥18 years; (3) mainly presenting with recurrent ischemic symptoms, including transient ischemic attack (TIA) and small cerebral infarction; (4) with a significant decrease in basal perfusion and reservoir capacity on preoperative brain single-photon emission computed tomography (SPECT) and significant perfusion decrease and delay on preoperative brain arterial spin-labeling (ASL)-magnetic resonance imaging (MRI); (5) with patent direct bypass confirmed on MR angiography before discharge; and (6) without preoperative

Received for publication December 4, 2024; accepted February 18, 2025.

From the *Department of Brain and Cognitive Engineering, Korea University; †Department of Neurosurgery, Seoul National University Hospital, Seoul National University College of Medicine; and ‡Department of Neurology, Korea University College of Medicine, Seoul, South Korea.

H.K., D.-J.K., and W.-S.C. contributed equally to this work.

Conflicts of interest and sources of funding: This work was supported by a grant from the Korea Health Technology R&D Project through the Korea Health Industry Development Institute (KHIDI) funded by the Ministry of Health & Welfare, Republic of Korea (grant number: HI17C1561), and the National Research Foundation of Korea (NRF) grant funded by the Korea government (MSIT) (No. 2022R1A2C1013205, No. RS-2024-00336744, and RS-2024-00414007). The authors have no conflicts of interest to declare.

Correspondence to: Dong-Joo Kim, PhD, E-mail: dongjookim@korea.ac.kr, Hakseung Kim, PhD, Email: mkhsm@korea.ac.kr, Department of Brain and Cognitive Engineering, Korea University, 145, Anam-ro, Seongbuk-gu, Seoul 02841, South Korea, and Won-Sang Cho, MD, PhD, Department of Neurosurgery, Seoul National University Hospital, Seoul National University College of Medicine, 101 Daehak-Ro, Jongno-Gu, Seoul 03080, South Korea, E-mail: nsdrcho@snu.ac.kr.

DOI: 10.1097/RLU.0000000000005850

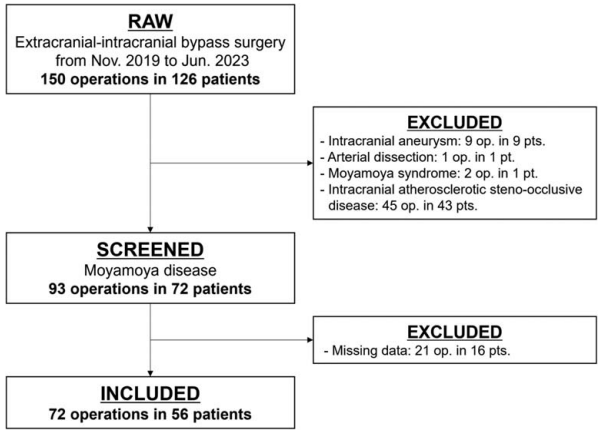

FIGURE 1. Consort diagram of the patient inclusion/exclusion process. op. indicates operation; pt(s)., patient(s).

major strokes that significantly confounded imaging analysis. This study was approved by the Institutional Review Board (approval number: H-2405-116-1537).

Surgical Procedure and Postoperative Management

The surgery was performed under general anesthesia induced by intravenous propofol and remifentanil. Combined bypass surgery involving both direct [superficial temporal artery (STA)-middle cerebral artery (MCA) anastomosis] and indirect (encephalo-duro-galeo-fascio-synangiosis) methods was performed. During surgery, arterial PCO_2 was maintained at 35–40 mm Hg, and the blood pressure was kept at the mean preoperative systolic blood pressure ± 15 mm Hg. Mild hypothermia, ~34 °C, was induced.

Postoperatively, the patients were normohydrated. The mean arterial pressure was maintained at the preoperative level ± 10 mm Hg, with a systolic pressure below 140 mm Hg. When CHS occurred, systolic pressure was maintained at ≤ 130 mm Hg. Hemoglobin was maintained between 10 and 11 g/dL. No additional medications, such as edaravone, minocycline, steroids, or antiplatelet agents, were administered. Details regarding the surgical procedure and postoperative care have been previously reported.[4,16]

Diagnosis of Postoperative CHS and Clinical Evaluation

The diagnostic criteria for postoperative CHS were as follows: (1) postoperative focal hyperperfusion detected on brain ASL-MRI or basal SPECT without evidence of newly developed cerebral infarction and intracranial hemorrhage; (2) clinical manifestations corresponding well with the topographic location of hyperperfusion, including headache, neurological deficits such as sensory, motor, language, and visual problems, altered mental status, and intracranial hemorrhage[4,8,11]; and (3) the aforementioned clinical symptoms different from the preoperative characteristics.

Preoperative clinical presentations included TIA, cerebral infarction, and intracranial hemorrhage. Other symptoms included involuntary movements, dizziness, and seizures. The neurological states of the operated patients were evaluated using the modified Rankin scale (mRS) preoperatively and at discharge.[22] In addition, preoperative hypertension and hematocrit were recorded.[21]

Preoperative ASL-MRI and SPECT Protocols

Preoperative basal and acetazolamide-challenged SPECT were conducted. Initially, patients at rest were administered 555 MBq of ^{99}mTc-hexamethylpropyleneamine oxime intravenously, followed by basal perfusion (BAS) imaging 5 minutes later. Ten minutes before BAS imaging completion, 20 mg of acetazolamide per kg body weight was injected intravenously, followed by an additional injection of 1110 MBq of ^{99}mTc-hexamethylpropyleneamine oxime. The second SPECT scan was performed 5 minutes after basal SPECT completion. In the second SPECT image, decay-corrected subtraction of BAS imaging was performed, defined as acetazolamide perfusion (ACZ) imaging. All protocol details were consistent with the previously reported details.[23] SPECT images were acquired using a triple-head camera (Prism 3000; Picker International) equipped with a low-energy, high-resolution fan-beam collimator. Forty step-and-shoot images were captured at 3-degree intervals for 20 seconds per step. SPECT images of BAS and ACZ (128×128 matrix) were reconstructed using Metz filter back-projection.

In the ASL sequence, a multiphase protocol was applied at various post-label delay times (1.00, 1.22, 1.48, 1.78, 2.15, 2.63, and 3.32 s) and effective labeling durations (0.22, 0.26, 0.30, 0.37, 0.48, 0.68, and 1.18 s), with a total scan duration of 3 minutes and 53 seconds. Specific ASL-MRI imaging parameters were as follows: repetition time, 6371 ms; echo time, 11.0 ms; flip angle, 111 degrees; field of view, 240×240; matrix, 128×128; section thickness, 6 mm; number of averages, 1; number of slices, 28; readout, 4 spiral arms×640 samples; and voxel resolution, 3.8×3.8×5.0 mm. ASL-MRI was performed using a 3.0 T scanner (Discovery 750; GE Healthcare) with a 32-channel head coil. To minimize potential errors due to differences in matrix size and slice spacing, the images were resampled and co-registered. From the data, conventional ASL-MRI [raw cerebral blood flow (rCBF) without knowledge of the transit time], transit time-corrected ASL-MRI maps [transit-corrected cerebral blood flow (tcCBF)], and transit time maps using the weighted delay method [transit delay (TD)] were computed. The ASL-MRI protocol followed previously reported methods.[11,24] SPECT and ASL-MRI examinations were conducted for all patients within 3 months before surgery.

Imaging Analysis

Based on a previous study,[25] a modified version of imaging analysis was used in this study. Seven regions of interest (ROIs) were used for preoperative ASL-MRI and SPECT imaging. Each ROI was measured in 4 axial planes: (1) orbitomeatal plane, (2) 34 mm above the orbitomeatal plane, (3) 51 mm above the orbitomeatal plane, and (4) 68 mm above the orbitomeatal plane. ROI diameters were 20 mm for both SPECT and MRI. ROIs were marked at the pons; lower frontal (lF), high frontal (hF), temporal (T), parietal (P), and occipital (O) cortices; and basal ganglia (BG) (Fig. 2). ROI values were calculated as average values within these areas. Only the operated hemispheres were analyzed. For ASL-MRI, the average ROI values for each area were used directly as feature values. In contrast, the perfusion states of BAS and ACZ imaging and CVR of each ROI on SPECT were semi-quantitatively calculated and compared to the values for the pons.[16,17] Table 1 lists the features derived from each modality. The preoperative Suzuki grade was evaluated using preoperative cerebral angiography.[1]

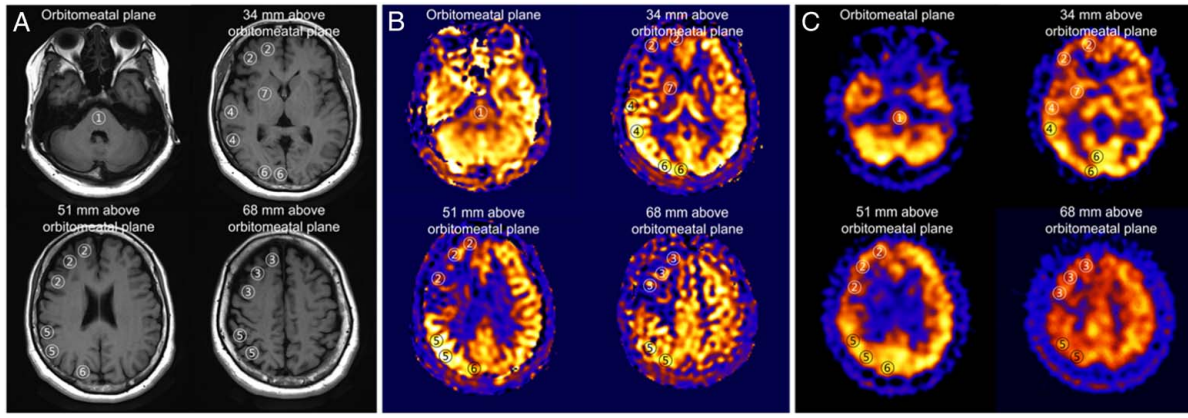

FIGURE 2. Regions of interest (ROIs) in each brain slice (orbitomeatal plane, orbitomeatal plane above 34 mm, orbitomeatal plane above 51 mm, and orbitomeatal plane above 68 mm). (A) T1 image; (B) ASL-MRI image; (C) SPECT image. 1 = pons, 2 = low frontal cortex, 3 = high frontal cortex, 4 = temporal cortex, 5 = parietal cortex, 6 = occipital cortex, and 7 = basal ganglia. ASL indicates arterial spin-labeling; MRI, magnetic resonance imaging; SPECT, single-photon emission computed tomography.

Basal Perfusion on SPECT

Semi-quantitative calculations of the BAS and ACZ images at each ROI were performed as follows.[25] The values for the 6 ROIs were divided by the values for the pons, resulting in the derivation of BAS_{Pons}_ROI and ACZ_{Pons}_ROI.

$$BAS_{Pons}\_ROI\ (\%) = \frac{BAS\_ROI}{BAS\_Pons} \times 100, \quad (1)$$

$$ACZ_{Pons}\_ROI\ (\%) = \frac{ACZ\_ROI}{ACZ\_Pons} \times 100. \quad (2)$$

CVR on SPECT

CVR, reflecting the physiological characteristics of the cerebral arteries that alter vessel diameters in response to stimuli, was also employed as a feature.[16,17,23] CVR is based on the relative ratio between an ROI and the pons as a reference as follows:

$$CVR\_ROI = \frac{ACZ\_ROI}{BAS\_ROI}, \quad (3)$$

$$CVR_{Pons}\_ROI\ (\%) = \frac{CVR\_ROI}{CVR\_Pons} \times 100. \quad (4)$$

Statistical Analysis

Continuous and categorical variables are presented as mean ± SD (range) and numbers (%), respectively. Outlier features that exceeded the 95% CI were replaced with the mean values. To handle unmeasured correlations between observations by including data from the same patient twice, which violated the assumption of independence, a generalized estimating equation (GEE) was applied in all analyses. Univariable analysis was conducted to assess the effect of each variable on CHS. The area under the receiver operating characteristic curve (AUROC) was derived based on the GEE model predictions. The cutoff value was determined using the Youden index. Multivariable analysis was performed to verify whether the trends observed in the univariable and AUROC analyses persisted after adjusting for clinical demographic characteristics. In all analyses, $P < 0.050$ was considered statistically significant. All statistical analyses were performed using SPSS software (version 25; IBM Corp.).

RESULTS

Demographic Information

Table 2 summarizes the demographic information. The mean age was 38.1 ± 10.3 years (range, 19–61 y), and 18.06% of the patients were male. All patients were right-

TABLE 1. Hemodynamic Features Derived From Preoperative Radiologic Data

Imaging modalities	Features according to regions
SPECT features	
BAS	BAS_{Pons}_lF, BAS_{Pons}_hF, BAS_{Pons}_T, BAS_{Pons}_P, BAS_{Pons}_O, BAS_{Pons}_BG,
ACZ	ACZ_{Pons}_lF, ACZ_{Pons}_hF, ACZ_{Pons}_T, ACZ_{Pons}_P, ACZ_{Pons}_O, ACZ_{Pons}_BG,
CVR	CVR_{Pons}_lF, CVR_{Pons}_hF, CVR_{Pons}_T, CVR_{Pons}_P, CVR_{Pons}_O, CVR_{Pons}_BG,
ASL-MRI features	
rCBF	rCBF_lF, rCBF_hF, rCBF_T, rCBF_P, rCBF_O, rCBF_BG
tcCBF	tcCBF_lF, tcCBF_hF, tcCBF_T, tcCBF_P, tcCBF_O, tcCBF_BG
TD	TD_lF, TD_hF, TD_T, TD_P, TD_O, TD_BG

ACZ indicates acetazolamide-challenged basal perfusion; ASL-MRI, arterial spin-labeling magnetic resonance imaging; BAS, basal perfusion; BG, basal ganglia; CVR, cerebrovascular reservoir capacity; hF, high frontal cortex; lF, lower frontal cortex; O, occipital cortex; P, parietal cortex; rCBF, raw cerebral blood flow; SPECT, single-photon emission computed tomography; T, temporal cortex; tcCBF, transit-corrected cerebral blood flow; TD, transit delay.

TABLE 2. Demographic Characteristics

	Total (n = 72)	Non-CHS group (n = 37)	CHS group (n = 35)	*P*
Age, y	38.1 ± 10.3 (19–61)	37.5 ± 9.4 (19–61)	38.7 ± 11.3 (21–60)	0.628
Males:Females	13:59 (18.1:81.9)	5:32 (13.5:86.5)	8:27 (22.9:77.1)	0.252
Clinical presentation				
Cerebral infarction	52 (72.2)	28 (75.7)	24 (68.6)	0.503
Transient ischemic attack	55 (76.4)	26 (70.3)	29 (82.9)	0.212
Intracerebral hemorrhage	7 (9.7)	6 (16.2)	1 (2.9)	0.008
Others	6 (8.3)	4 (10.8)	2 (5.7)	0.405
Operated hemisphere				0.080
Left	32 (44.4)	13 (35.1)	19 (54.3)	
Right	40 (55.6)	24 (64.9)	16 (45.7)	
Suzuki grade	4.14 ± 1.1 (2–6)	4.27 ± 0.9 (2–6)	4.00 ± 1.2 (2–6)	0.320
2	7 (9.7)	2 (5.4)	5 (14.3)	
3	10 (13.9)	4 (10.8)	6 (17.1)	
4	28 (38.9)	15 (40.5)	13 (37.1)	
5	20 (27.8)	14 (37.8)	6 (17.1)	
6	7 (9.7)	2 (5.4)	5 (14.3)	
Hypertension	23 (31.9)	9 (25.7)	14 (37.8)	0.282
Hematocrit	38.6 ± 4.1 (24.9–46.5)	38.6 ± 4.3 (24.9–45.9)	38.7 ± 3.9 (31.4–46.5)	0.896
Modified Rankin scale score				
Preoperatively	1.3 ± 0.7 (0–4)	1.2 ± 0.8 (0–4)	1.4 ± 0.6 (0–3)	0.158
At discharge	1.1 ± 0.8 (0–4)	1.0 ± 1.0 (0–4)	1.2 ± 0.7 (0–4)	0.402
Postoperative CHS				
Initiation, days after surgery	—	—	3.9 ± 2.5 (0–9)	
Duration, days	—	—	8.5 ± 4.0 (0–17)	

Continuous and categorical variables are presented as mean ± SD (range) and number (%), respectively. Group comparisons were performed using a generalized estimating equation. The % was calculated with the number of hemispheres as the denominator.

CHS indicates cerebral hyperperfusion syndrome.

handed. No significant between-group differences were observed in any variable except intracerebral hemorrhage (CHS: 2.9% vs. non-CHS: 16.2%, $P = 0.008$). Postoperative CHS occurred in 35 cases (48.61%), with a mean initiation of 3.9 ± 2.5 days (range, 0–9 d) after surgery and a mean duration of 8.5 ± 4.0 days (range, 0–17 d). All direct bypasses were patent and confirmed by MR angiography within 24 hours before discharge. Postoperative complications other than CHS occurred in 9 cases (12.5%), including transient symptomatic cortical infarction (n = 2), asymptomatic cortical infarction (n = 1), transiently symptomatic subarachnoid hemorrhage (n = 1), asymptomatic subgaleal hematoma (n = 1), transiently symptomatic seizure (n = 1), levetiracetam-related psychosis (n = 2), and pulmonary thromboembolism (n = 1). All patients with postoperative complications recovered well, except for 1 patient with pulmonary thromboembolism.

Univariable and AUROC Analysis Between CHS and Non-CHS Groups

Table 3 presents the hemodynamic features from SPECT and ASL-MRI that demonstrated statistical significance in the univariable analysis. CVR_{Pons}_T, CVR_{Pons}_lF, CVR_{Pons}_hF, ACZ_{Pons}_T, rCBF_hF, CVR_{Pons}_P, ACZ_{Pons}_P, and tcCBF_hF demonstrated statistically significant between-group differences (GEE, all $P < 0.05$). Among these, CVR_{Pons}_T, CVR_{Pons}_lF, and CVR_{Pons}_hF demonstrated significant predictive power for postoperative CHS (AUROC, $P = 0.023$, 0.028, and 0.039, respectively). The

TABLE 3. Effect and Predictive Capacity of Hemodynamic Features Derived From SPECT and ASL-MRI on Postoperative CHS

Feature	Generalized estimation equation			AUROC	
	Odds ratio (95% CI)	*P*	AUROC (95% CI)	Cutoff	*P*
CVR_{Pons}_T	0.990 (0.984–0.996)	0.001	0.656 (0.530–0.783)	84.749	0.023
CVR_{Pons}_lF	0.991 (0.986–0.996)	0.000	0.650 (0.524–0.777)	91.943	0.028
CVR_{Pons}_hF	0.990 (0.983–0.998)	0.011	0.642 (0.513–0.770)	88.732	0.039
ACZ_{Pons}_T	0.495 (0.259–0.947)	0.034	0.633 (0.505–0.761)	117.558	0.052
rCBF_hF	0.997 (0.995–1.000)	0.026	0.623 (0.492–0.754)	99.010	0.072
CVR_{Pons}_P	0.990 (0.982–0.998)	0.013	0.611 (0.480–0.741)	84.817	0.106
ACZ_{Pons}_P	0.556 (0.373–0.829)	0.004	0.608 (0.478–0.739)	126.023	0.113
tcCBF_hF	0.997 (0.994–1.000)	0.038	0.599 (0.468–0.731)	115.665	0.148

ACZ indicates acetazolamide-challenged basal perfusion; AUROC, area under the receiver operating characteristic curve; CHS, cerebral hyperperfusion syndrome; CI, confidence interval; CVR, cerebrovascular reservoir capacity; hF, higher frontal cortex; lF, lower frontal cortex; P, parietal cortex; rCBF, raw cerebral blood flow; T, temporal cortex; tcCBF, transit-corrected CBF.

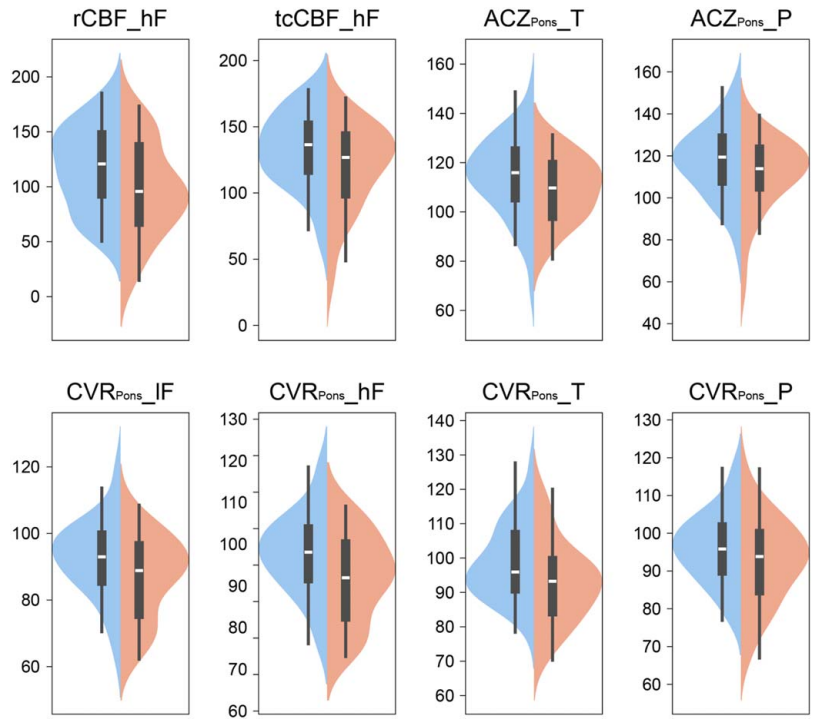

FIGURE 3. Violin and box plots comparing inter-group hemodynamic features with a significant impact on postoperative CHS. The red and blue distributions represent the CHS and non-CHS groups, respectively. ACZ indicates acetazolamide-challenged basal perfusion; CVR, cerebrovascular reservoir capacity; hF, higher frontal cortex; lF, lower frontal cortex; P, parietal cortex; rCBF, raw cerebral blood flow; T, temporal cortex; tcCBF, transit-corrected cerebral blood flow.

violin plot and AUROC curve for the specified variables are shown in Figures 3 and 4, respectively.

Multivariable Analysis Between the CHS and Non-CHS Groups

In the multivariable analysis adjusted for clinical data (Table 4), the likelihood of developing postoperative CHS increased with lower CVR_{Pons}_T [odds ratio (OR) (95% CI), 0.94 (0.88–0.99); $P = 0.046$], higher preoperative mRS score [3.25 (1.35–7.79); $P = 0.008$], and left-sided surgery [4.06 (1.11–14.90); $P = 0.034$]. The prediction accuracy of the GEE model was 81.94%. Based on the standardized coefficients, preoperative mRS, left-operated hemisphere, and CVR_{Pons}_T, in that order, were the most influential predictors in the model.

DISCUSSION

Despite various studies attempting to predict postoperative CHS, a key factor influencing surgical outcomes after direct bypass for MMD, no consistent predictive factors have been identified. Impaired cerebral autoregulation is considered the most probable cause, but its association has only been reported in our recent studies using transcranial Doppler[20] and dynamic contrast-enhanced MRI.[11] In research utilizing radiologic data, only 1 study by Sato et al[17] indirectly referenced the relationship between CHS and low preoperative CVR as a hemodynamic factor. Accordingly, this study aimed to identify hemodynamic predictors of postoperative CHS by analyzing features derived from preoperative SPECT and ASL-MRI. The findings revealed that poor preoperative CVR in the temporal and frontal cortices was associated with an increased risk of CHS. Even after adjusting for confounding factors based on demographic information, a poorer CVR_{Pons}_T remained a significant hemodynamic factor. Therefore, this study is meaningful as it confirmed CVR as an important hemodynamic factor through preoperative imaging and localized it to a specific temporal cortex region. Moreover, poor preoperative neurological status and anastomosis in the dominant hemisphere were significant factors influencing CHS occurrence, solidifying their role as predictors, as previously reported.[12–15]

Based on the theory that impaired cerebral autoregulation is the mechanism underlying CHS, it speculated that lower preoperative CBF and CVR increase the likelihood of postoperative CHS.[17,26,27] CVR reflects the intrinsic ability of the brain to adjust the diameter of the cerebral arteries in response to acetazolamide administration, primarily indicating its vasodilatory capacity.[16,17,23] Normal blood vessels dilate in response to acetazolamide administration, accommodating increased blood flow. In contrast, MMD-related vessels, which are persistently dilated due to chronic ischemia, do not dilate further, even after administration. Rather, blood is stolen by the expansion of vessels in less ischemic or normal areas, leading to a reduction in CVR. Therefore, the CVR on SPECT serves as an indicator of cerebral autoregulation. One proposed mechanism of postoperative CHS is the inability of the brain to respond adequately to sudden increases in blood flow.[17] Given this background, patients with preoperative impairments in autoregulation and CVR are presumed to be at a higher

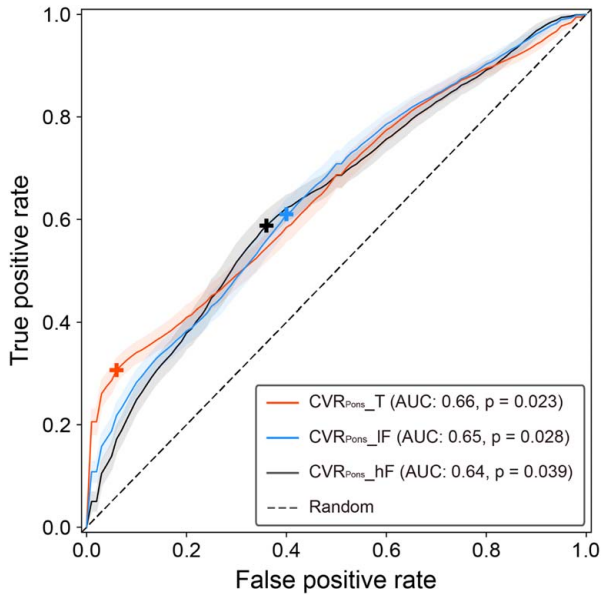

FIGURE 4. AUROC plots showing the predictive capacity of features significantly associated with postoperative CHS. The cross marker indicates the cutoff point. AUROC indicates area under the receiver operating characteristic curve; CHS, cerebral hypoperfusion syndrome; CVR, cerebrovascular reservoir capacity; hF, higher frontal cortex; lF, lower frontal cortex; T, temporal cortex.

risk of CHS, as the brain may not adequately manage the elevated blood flow.

The significant indicators in the univariable GEE and AUROC analyses were CVR_{Pons}_T, CVR_{Pons}_lF, and CVR_{Pons}_hF (cutoff values, 84.7, 91.9, and 88.7, respectively). Of these, CVR_{Pons}_T was the only indicator that retained significance in the multivariable GEE, indicating that a lower value increases the likelihood of CHS occurrence [OR (95% CI), 0.990 (0.980–0.999)]. The temporal cortex receives collateral blood supply from branching arteries of the posterior cerebral artery (PCA), in addition to its primary supply from the MCA. Ischemia in the temporal cortex, characterized by low CBF and CVR, typically results from inadequate blood supply from both the PCA and MCA. Thus, temporal cortex ischemia can indicate that at least part of the MCA territory is likely experiencing severe ischemia. PCA involvement occurs in approximately 30% of patients with MMD,[15,28] and postoperative ischemic events are more likely to occur in patients with PCA involvement. Taken together, patients with poor MCA and PCA collaterals, along with a preoperative CVR_{Pons}_T value below 84.75%, would highly likely face a greater risk of CHS, requiring careful postoperative observation and timely intervention.

Unlike the findings of the univariate analysis, mRS and operated hemisphere demonstrated statistical significance in the multivariate analysis. Higher preoperative mRS scores, which indicate a severe neurological status, were positively correlated with CHS occurrence [OR (95% CI), 1.178 (1.045–1.328)], which is consistent with previous studies.[12,15] In addition, it was confirmed that CHS occurred more frequently when surgery was performed in the left hemisphere [OR (95% CI), 1.245 (1.054–1.471)]. All the participants in this study cohort were right-handed; thus, it was assumed that symptoms manifested more frequently when the dominant hemisphere, which may be functionally more important and sensitive, underwent hyperperfusion.[13] The standardized coefficients for mRS and the left hemisphere were 2.448 and 2.226, respectively, indicating that mRS is a relatively more important predictor of CHS.

SPECT is widely performed to evaluate the hemodynamic status, but it has limitations such as complications related to acetazolamide,[14,29] x-ray exposure, and the need for specialized facilities for nuclear medicine examinations. Recognizing the challenges of repeated SPECT acquisitions, some researchers have attempted to replace SPECT with non-contrast MRI.[30,31] Accordingly, the present study analyzed several features to ascertain whether SPECT or MRI is more effective in predicting postoperative CHS. Although the same number of features and regions were analyzed, statistical significance was primarily observed in SPECT, likely due to the lower accuracy of ASL-MRI. ASL-MRI provides a sharper gray-white matter boundary than SPECT. In the cortex, white matter signals may appear relatively as filling defects, leading to consistently lower ROI measurements on ASL-MRI than those on SPECT. Furthermore, SPECT reflects relatively cumulative brain

TABLE 4. Multivariable Generalized Estimating Equation Analysis for Predicting Postoperative CHS

Feature	VIF	Standardized coefficients	Odds ratio (95% CI)	*P*
Age	1.249			
Sex	2.188			
Cerebral infraction	3.567			
Transient ischemic attack	2.693			
Intracerebral hemorrhage	2.510			
Other symptoms	2.496			
Left-operated hemisphere	1.109	2.114	4.064 (1.108–14.904)	0.034
Preoperative Suzuki grade	1.340			
Preoperative modified Rankin scale	1.146	2.640	3.248 (1.354–7.791)	0.008
Preoperative hypertension	1.524			
Preoperative hematocrit	1.623			
CVR_{Pons}_T	2.109	−1.997	0.938 (0.880–0.999)	0.046
CVR_{Pons}_lF	2.776			
CVR_{Pons}_hF	2.693			

CHS indicates cerebral hyperperfusion syndrome; CVR, cerebrovascular reservoir capacity; hF, higher frontal cortex; lF, lower frontal cortex; T, temporal cortex; VIF, variance inflation factor.

parenchymal perfusion, whereas ASL-MRI captures temporary intravascular perfusion. Thus, ASL-MRI has inherent limitations in representing time-delay or true brain perfusion, despite efforts to develop corrected imaging techniques. This study does not indicate a limitation of ASL-MRI but rather suggests the need for further protocol development. For instance, implementing ASL-MRI with the injection of a specific contrast agent, developing new ASL-MRI protocols, or advancing other hemodynamic perfusion MRI techniques should be pursued.

In general, the prevalence of CHS is reported to be approximately 20%.[32] However, nearly half of the hemispheres in this study experienced postoperative CHS. Contributing factors include strict surgical indications for the patients with hemodynamic compromise and clinical symptoms; a high proportion (76.4%) of patients with advanced Suzuki grades 4–6; and the selection of recipient arteries primarily supplying eloquent areas. Most notably, this study is subject to selection bias because patients were included based on specific criteria during a certain period rather than being consecutively enrolled. In addition, well-known predictors of postoperative CHS (eg, age,[12] clinical presentation,[12,15] Suzuki grade,[13,15] hypertension,[21] hematocrit,[21] and CBF[11]) were included in the analysis; however, they did not yield statistical significance.

This study has some limitations. First, this was a retrospective study conducted at a single center. Second, the sample size of patients with MMD was limited; selection bias might have been introduced because patients were not consecutively enrolled. Nonetheless, this study was designed to compare CHS and non-CHS groups, and no statistical differences were observed in the baseline demographics. Third, the ROI was manually set. Therefore, the findings could be subjected to relative bias, rendering their implementation in clinical settings difficult. Fourth, the relatively low SPECT resolution renders it difficult to accurately define the ROI. To address this issue, the ROI was identified on the MRI template to measure the feature values on SPECT.

In conclusion, univariable analysis of hemodynamic features identified low CVR in the lF, hF, and T cortices as a risk factor for postoperative CHS. Multivariable analysis, incorporating both clinical and hemodynamic features, indicated that low CVR in the temporal cortex, high preoperative mRS, and anastomosis in the dominant hemisphere were risk factors. The present study directly demonstrated that the hemodynamic factor, CVR_{Pons_T}, derived from preoperative SPECT was effective in predicting CHS. These findings are expected to aid in the management of postoperative CHS through preoperative predictions. Multicenter and prospectively designed studies need to be conducted in the future to better capture the characteristics of the CHS population. In addition to statistical approaches, emerging artificial intelligence techniques can enhance the accuracy of predicting postoperative CHS.

REFERENCES

1. Suzuki J, Kodama N. Moyamoya disease—a review. *Stroke*. 1983;14:104–109.
2. Guzman R, Lee M, Achrol A, et al. Clinical outcome after 450 revascularization procedures for moyamoya disease. *J Neurosurg*. 2009;111:927–935.
3. Kim SK, Cho BK, Phi JH, et al. Pediatric moyamoya disease: an analysis of 410 consecutive cases. *Ann Neurol*. 2010;68: 92–101.
4. Cho W-S, Kim JE, Kim CH, et al. Long-term outcomes after combined revascularization surgery in adult moyamoya disease. *Stroke*. 2014;45:3025–3031.
5. Takahashi JC, Funaki T, Houkin K, et al. Significance of the hemorrhagic site for recurrent bleeding: prespecified analysis in the Japan Adult Moyamoya Trial. *Stroke*. 2016; 47:37–43.
6. Fujimura M, Kaneta T, Mugikura S, et al. Temporary neurologic deterioration due to cerebral hyperperfusion after superficial temporal artery-middle cerebral artery anastomosis in patients with adult-onset moyamoya disease. *Surg Neurol*. 2007;67:273–282.
7. Cho W-S, Lee H-Y, Kang H-S, et al. Symptomatic cerebral hyperperfusion on SPECT after indirect revascularization surgery for Moyamoya disease. *Clin Nucl Med*. 2013;38: 44–46.
8. Kim JE, Oh CW, Kwon O-K, et al. Transient hyperperfusion after superficial temporal artery/middle cerebral artery bypass surgery as a possible cause of postoperative transient neurological deterioration. *Cerebrovasc Dis*. 2008;25:580–586.
9. Nomura S, Yamaguchi K, Ishikawa T, et al. Factors of delayed hyperperfusion and the importance of repeated cerebral blood flow evaluation for hyperperfusion after direct bypass for moyamoya disease. *World Neurosurg*. 2018;118: e468–e472.
10. Research Committee on the Pathology and Treatment of Spontaneous Occlusion of the Circle of Willis; Health Labour Sciences Research Grant for Research on Measures for Infractable Diseases. Guidelines for diagnosis and treatment of moyamoya disease (spontaneous occlusion of the circle of Willis). *Neurol Med Chir (Tokyo)*. 2012;52:245–266.
11. Lee K, Yoo R-E, Cho W-S, et al. Blood-brain barrier disruption imaging in postoperative cerebral hyperperfusion syndrome using DCE-MRI. *J Cereb Blood Flow Metab*. 2024; 44:345–354.
12. Pang CH, Lee SU, Lee Y, et al. Prediction of hemorrhagic cerebral hyperperfusion syndrome after direct bypass surgery in adult nonhemorrhagic moyamoya disease: combining quantitative parameters on RAPID perfusion CT with clinically related factors. *J Neurosurg*. 2022;138:683–692.
13. Shi Z, Wu L, Wang Y, et al. Intraoperative hemodynamics of parasylvian cortical arteries for predicting postoperative symptomatic cerebral hyperperfusion after direct revascularization in patients with moyamoya disease: a preliminary study. *J Clin Med*. 2023;12:3855.
14. Hwang J, Yang H, Lee H, et al. Predictive factors of symptomatic cerebral hyperperfusion after superficial temporal artery-middle cerebral artery anastomosis in adult patients with moyamoya disease. *Br Anaesth*. 2013;110:773–779.
15. Zhao M, Deng X, Zhang D, et al. Risk factors for and outcomes of postoperative complications in adult patients with moyamoya disease. *J Neurosurg*. 2018;130:531–542.
16. Lee SH, Cho W-S, Lee HC, et al. The ivy sign as a radiological marker for follow-up of postoperative cerebral perfusion status in adult moyamoya disease. *J Neurosurg*. 2023;1:1–8.
17. Sato S, Kojima D, Shimada Y, et al. Preoperatively reduced cerebrovascular contractile reactivity to hypocapnia by hyperventilation is associated with cerebral hyperperfusion syndrome after arterial bypass surgery for adult patients with cerebral misery perfusion due to ischemic moyamoya disease. *J Cereb Blood Flow Metab*. 2018;38:1021–1031.
18. Ogasawara K, Inoue T, Kobayashi M, et al. Pretreatment with the free radical scavenger edaravone prevents cerebral hyperperfusion after carotid endarterectomy. *Neurosurgery*. 2004;55: 1060–1067.
19. Fujimura M, Niizuma K, Inoue T, et al. Minocycline prevents focal neurological deterioration due to cerebral hyperperfusion after extracranial-intracranial bypass for moyamoya disease. *Neurosurgery*. 2014;74:163–170.
20. Kim JH, Hong N, Kim H, et al. Autoregulatory dysfunction in adult Moyamoya disease with cerebral hyperperfusion syndrome after bypass surgery. *Sci Rep*. 2024;14:26451.

21. Xu D, Guo J, Zheng B, et al. Risk factors for cerebral hyperperfusion syndrome after combined revascularization in adult patients with Moyamoya disease. *Curr Neurovasc Res*. 2023;20:623–629.
22. Uyttenboogaart M, Stewart RE, Vroomen PC, et al. Optimizing cutoff scores for the Barthel index and the modified Rankin scale for defining outcome in acute stroke trials. *Stroke*. 2005; 36:1984–1987.
23. Lee H-Y, Paeng JC, Lee DS, et al. Efficacy assessment of cerebral arterial bypass surgery using statistical parametric mapping and probabilistic brain atlas on basal/acetazolamide brain perfusion SPECT. *J Nucl Med*. 2004; 45:202–206.
24. Yun TJ, Sohn C-H, Yoo R-E, et al. Transit time corrected arterial spin labeling technique aids to overcome delayed transit time effect. *Neuroradiology*. 2018;60:255–265.
25. Hoshi H, Ohnishi T, Jinnouchi S, et al. Cerebral blood flow study in patients with moyamoya disease evaluated by IMP SPECT. *J Nucl Med*. 1994;35:44–50.
26. Hayashi K, Horie N, Suyama K, et al. Incidence and clinical features of symptomatic cerebral hyperperfusion syndrome after vascular reconstruction. *World Neurosurg*. 2012;78:447–454.
27. Kaku Y, Yoshimura S-i, Kokuzawa J. Factors predictive of cerebral hyperperfusion after carotid angioplasty and stent placement. *AJNR Am J Neuroradiol*. 2004;25: 1403–1408.
28. Ge P, Zhang Q, Ye X, et al. Long-term outcome after conservative treatment and direct bypass surgery of moyamoya disease at late Suzuki stage. *World Neurosurg*. 2017;103:283–290.
29. Lee JY, Phi JH, Wang K-C, et al. Neurocognitive profiles of children with Moyamoya disease before and after surgical intervention. *Cerebrovasc Dis*. 2011;31:230–237.
30. Noguchi T, Kawashima M, Nishihara M, et al. Noninvasive method for mapping CVR in moyamoya disease using ASL-MRI. *Eur J Radiol*. 2015;84:1137–1143.
31. Kawano T, Ohmori Y, Kaku Y, et al. Prolonged mean transit time detected by dynamic susceptibility contrast magnetic resonance imaging predicts cerebrovascular reserve impairment in patients with moyamoya disease. *Cerebrovasc Dis*. 2016;42: 131–138.
32. Yu J, Zhang J, Li J, et al. Cerebral hyperperfusion syndrome after revascularization surgery in patients with moyamoya disease: systematic review and meta-analysis. *World Neurosurg*. 2020;135:357–366. e4.